RESEARCH ARTICLE

EspZ of Enteropathogenic and Enterohemorrhagic *Escherichia coli* Regulates Type III Secretion System Protein Translocation

Cedric N. Berger,[a] Valerie F. Crepin,[a] Kobi Baruch,[b] Aurelie Mousnier,[a] Ilan Rosenshine,[b] and Gad Frankel[a]

Centre for Molecular Bacteriology and Infection, Division of Cell and Molecular Biology, Imperial College London, London, United Kingdom,[a] and Department of Microbiology and Molecular Genetics, IMRIC, The Hebrew University of Jerusalem, Faculty of Medicine, Jerusalem, Israel[b]

ABSTRACT **Translocation of effector proteins via a type III secretion system (T3SS) is a widespread infection strategy among Gram-negative bacterial pathogens. Each pathogen translocates a particular set of effectors that subvert cell signaling in a way that suits its particular infection cycle. However, as effector unbalance might lead to cytotoxicity, the pathogens must employ mechanisms that regulate the intracellular effector concentration. We present evidence that the effector EspZ controls T3SS effector translocation from enteropathogenic (EPEC) and enterohemorrhagic (EHEC) *Escherichia coli*. Consistently, an EPEC *espZ* mutant is highly cytotoxic. Following ectopic expression, we found that EspZ inhibited the formation of actin pedestals as it blocked the translocation of Tir, as well as other effectors, including Map and EspF. Moreover, during infection EspZ inhibited effector translocation following superinfection. Importantly, while EspZ of EHEC O157:H7 had a universal "translocation stop" activity, EspZ of EPEC inhibited effector translocation from typical EPEC strains but not from EHEC O157:H7 or its progenitor, atypical EPEC O55:H7. We found that the N and C termini of EspZ, which contains two transmembrane domains, face the cytosolic leaflet of the plasma membrane at the site of bacterial attachment, while the extracellular loop of EspZ is responsible for its strain-specific activity. These results show that EPEC and EHEC acquired a sophisticated mechanism to regulate the effector translocation.**

IMPORTANCE **Enteropathogenic *Escherichia coli* (EPEC) and enterohemorrhagic *E. coli* (EHEC) are important diarrheal pathogens responsible for significant morbidity and mortality in developing countries and the developed world, respectively. The virulence strategy of EPEC and EHEC revolves around a conserved type III secretion system (T3SS), which translocates bacterial proteins known as effectors directly into host cells. Previous studies have shown that when cells are infected in two waves with EPEC, the first wave inhibits effector translocation by the second wave in a T3SS-dependent manner, although the factor involved was not known. Importantly, we identified EspZ as the effector responsible for blocking protein translocation following a secondary EPEC infection. Interestingly, we found that while EspZ of EHEC can block protein translocation from both EPEC and EHEC strains, EPEC EspZ cannot block translocation from EHEC. These studies show that EPEC and EHEC employ a novel infection strategy to regulate T3SS translocation.**

Received 31 August 2012 **Accepted** 4 September 2012 **Published** 2 October 2012

Citation Berger CN, et al. 2012. EspZ of enteropathogenic and enterohemorrhagic *E. coli* regulates type III secretion system protein translocation. mBio 3(5):e00317-12 doi: 10.1128/mBio.00317-12.

Editor Philippe Sansonetti, Institut Pasteur

Address correspondence to Gad Frankel, g.frankel@imperial.ac.uk.

Type III secretion systems (T3SS) are nanosyringes used by a large number of Gram-negative pathogenic bacteria of human, animals and plants (e.g., *Salmonella*, *Shigella*, *Yersinia*, *Pseudomonas*, *Xanthomonas*, *Chlamydia*, enteropathogenic *Escherichia coli*, and enterohemorrhagic *E. coli*) to translocate effector proteins directly from the bacterial cytosol into eukaryotic cells (reviewed in reference 1). The T3SS is embedded in the bacterial cell wall and consists of many different proteins and hundreds of individual subunits. The secretion apparatus is comprised of a basal body (consisting of stacked rings joined by a central rod) and an external "needle" (2). At the other end of the T3SS are components of the translocon, which directly interact with the eukaryotic membrane to form a translocation pore and a contiguous secretion channel between the bacterial and eukaryotic cytosol (reviewed in reference 3). A cytoplasmic ATPase, related to the catalytic subunits of bacterial F_oF_1 ATPases, energizes, via a proton motive force, effector protein translocation. Following translocation, the effectors target different organelles and signaling pathways, which define the infection strategy of each pathogen (reviewed in reference 4).

The multifunctional nature of the effectors and the fact that they can exhibit either synergistic or antagonistic activities suggests that the timing of their translocation has to be tightly coordinated. This is achieved at different levels, from the magnitude and timing of gene expression in the bacterial cell (5) to a hierarchy of effector protein translocation (6). Indeed, real-time analysis of effector translocation in enteropathogenic *E. coli* (EPEC) revealed a distinct order of protein translocation (7). Moreover, these studies showed that adherent EPEC can inhibit protein translocation from a second wave of infecting bacteria in a T3SS-

dependent manner (7), although the effector involved in this phenomenon was not known.

EPEC and enterohemorrhagic *E. coli* (EHEC) are important human pathogens. While EPEC strains cause bacterial pediatric diarrhea and mortality in developing countries (8), EHEC strains, particularly those belonging to serotype O157:H7, are associated with food-born outbreaks in developed countries, causing abdominal pain, nonbloody or bloody diarrhea, and, in about 10% of patients, hemolytic uremic syndrome (HUS) (9). Although they cause somewhat different diseases, EPEC and EHEC colonize the gut mucosa via formation of attaching-and-effacing (A/E) lesions, which are characterized by intimate attachment of the bacteria to the apical membrane of enterocytes and effacement of the brush border microvilli (10). *In vitro*, the hallmark of EPEC and EHEC infection is formation of actin-rich pedestals (11). Formation of A/E lesions *in vivo* and actin pedestals *in vitro* is dependent on the locus of enterocyte effacement (LEE) pathogenicity island (12). The LEE encodes transcriptional regulators, the adhesin intimin (13), a T3SS (14-16), chaperones, and seven effectors (Tir, Map, EspF, EspZ, EspH, EspB, and EspG) (reviewed in reference 17). Translocated Tir serves as an intimin receptor (18); intimin-Tir interaction is essential for A/E lesion and pedestal formation (19). Moreover, Tir (20) and EspH (21) downregulate filopodia that are triggered at early stages of infection by the LEE-encoded effector Map (20). At later stages of infection, Map traffics to the mitochondria (22). Similarly, the LEE-encoded effector EspF also targets the mitochondria, promoting mitochondrial dysfunction and apoptosis (reviewed in reference 17). In addition, EPEC and EHEC strains translocate multiple non-LEE-encoded effectors with diverse activities, which are encoded by genes carried on prophages and pathogenicity islands that are scattered around the chromosome (17, 23). The LEE-encoded effector EspZ (24) is a 98-amino-acid effector consisting of an N-terminal translocation signal (20 amino acids) (25) and two transmembrane domains (TMDs) that target it to the plasma membrane of infected cells (24). Importantly, an EPEC *espZ* mutant exhibits a high level of cytotoxicity (4). The aim of this study was to investigate the cytoprotection activity of EspZ.

RESULTS

An *espZ* EPEC mutant is cytotoxic. To determine the role of EspZ during infection, HeLa cells were infected for 3 h with the wild-type EPEC strain E2348/69, E2348/69 Δ*espZ*, and the complemented mutant. Whereas only few cells infected with wild-type E2348/69 or with the complemented Δ*espZ* strain detached from the monolayer, less than 30% of cells infected with E2348/69 Δ*espZ* remained attached at the end of the incubation period (Fig. 1A and B). DNA staining, performed following 1 h of infection, revealed that deletion of *espZ* resulted in nuclear condensation (nucleus $<100\ \mu m^2$) in 70% of cells. In contrast, nuclear condensation was seen in only 10 to 20% of the uninfected control cells or cells infected with wild-type E2348/69 or the complemented mutant (Fig. 1C and D).

To establish if the plasma membrane integrity was compromised during infection with the *espZ* mutant, cells were infected with wild-type E2348/69, E2348/69 Δ*espZ*, and the complemented mutant for 30 min, washed, and incubated with propidium iodide (PI). Accumulation of PI in cells was then monitored by live-cell imaging for 30 min. While no accumulation of PI was observed in uninfected cells (see Fig. S1A) or in cells infected with wild-type (data not shown) and complemented (see Fig. S1C) strains, the number of cells with red nuclei increased when cells were infected with E2348/69 Δ*espZ* (see Fig. S1B), suggesting that the plasma membrane was permeabilized.

We next investigated the level of lactate dehydrogenase (LDH) release following 2 h of infection of HeLa cells with wild-type E2348/69, E2348/69 Δ*espZ*, or the complemented mutant. Infection with E2348/69 Δ*escN* (defective in T3SS) was used as a control. Less than 10% of the total LDH was found in the supernatants of uninfected cells and cells infected with the wild type, the Δ*escN* mutant, and the Δ*espZ* complemented mutant. In contrast, more than 40% of the total LDH was released from cells infected with E2348/69 Δ*espZ* (Fig. 1E). This result suggests that the cytotoxicity is dependent on effector translocation and is mitigated by EspZ, confirming a previous report (4).

In order to determine whether the observed cell loss and LDH release seen following infection with E2348/69 Δ*espZ* were due to caspase-dependent apoptosis, we conducted infections in the presence of the global caspase inhibitor zVAD-FMK (carbobenzoxy-valyl-alanyl-aspartyl-[*O*-methyl]-fluoromethylketone). Cells pretreated with zVAD-FMK prior to infection with E2348/69 Δ*espZ* showed levels of cell detachment (see Fig. S2 in the supplemental material) and LDH release (Fig. 1E) similar to those of untreated cells infected with E2348/69 Δ*espZ*, suggesting that caspases are not involved in cytotoxicity. Taken together, these data suggest that the *espZ* mutant induces type III cell death (oncosis), characterized by nuclear condensation, rapid membrane permeabilization (IP accumulation in the cells), and cellular swelling (LDH release), independently of caspase activation.

Translocated EspZ is localized at the bacterial attachment site. EspZ, which localizes at the EPEC attachment site during infection of epithelial cells, is predicted to contain two TMDs (4, 24). In order to determine the localization and topology of EspZ, we fused a Myc tag to the N terminus (Myc-EspZ) and a tandem four-hemagglutinin (HA) tag epitope to the C terminus (EspZ-HA_4) and replaced the putative loop between the two TMDs with an HA tag ($EspZ_{Loop/HA}$). In order to localize EspZ during infection, HeLa cells were infected with wild-type E2348/69, E2348/69 Δ*espZ*, E2348/69 Δ*espZ* expressing Myc-EspZ, E2348/69 Δ*espZ* expressing EspZ-HA_4, or E2348/69 Δ*espZ* expressing $EspZ_{Loop/HA}$. E2348/69 Δ*escN* expressing EspZ-HA_4 was used as a negative control. Immunofluorescence revealed strong $EspZ_{Loop/HA}$ staining only inside the bacteria and cytotoxicity following infection with Δ*espZ* expressing $EspZ_{Loop/HA}$, suggesting that replacement of the loop abolished EspZ translocation and therefore prohibited further investigation. In contrast, both Myc-EspZ and EspZ-HA_4 were translocated and seen at the bacterial attachment sites (see Fig. S3A in the supplemental material), but only after permeabilization (see Fig. S3B). Moreover, while E2348/69 Δ*espZ* induced a large LDH release, the levels of LDH in the supernatants of cells infected with E2348/69 Δ*espZ* expressing Myc-EspZ or E2348/69 Δ*espZ* expressing EspZ-HA_4 were equivalent to those in uninfected cells and cells infected with wild-type E2348/69 (data not shown), confirming that Myc-EspZ and EspZ-HA_4 were functional. No specific EspZ staining was seen in cells infected with E2348/69 Δ*escN* expressing EspZ-HA_4 (see Fig. S3B). These results suggest that both the N and C termini of EspZ are cytosolic and therefore that EspZ integrates into the plasma membrane in a hairpin loop topology.

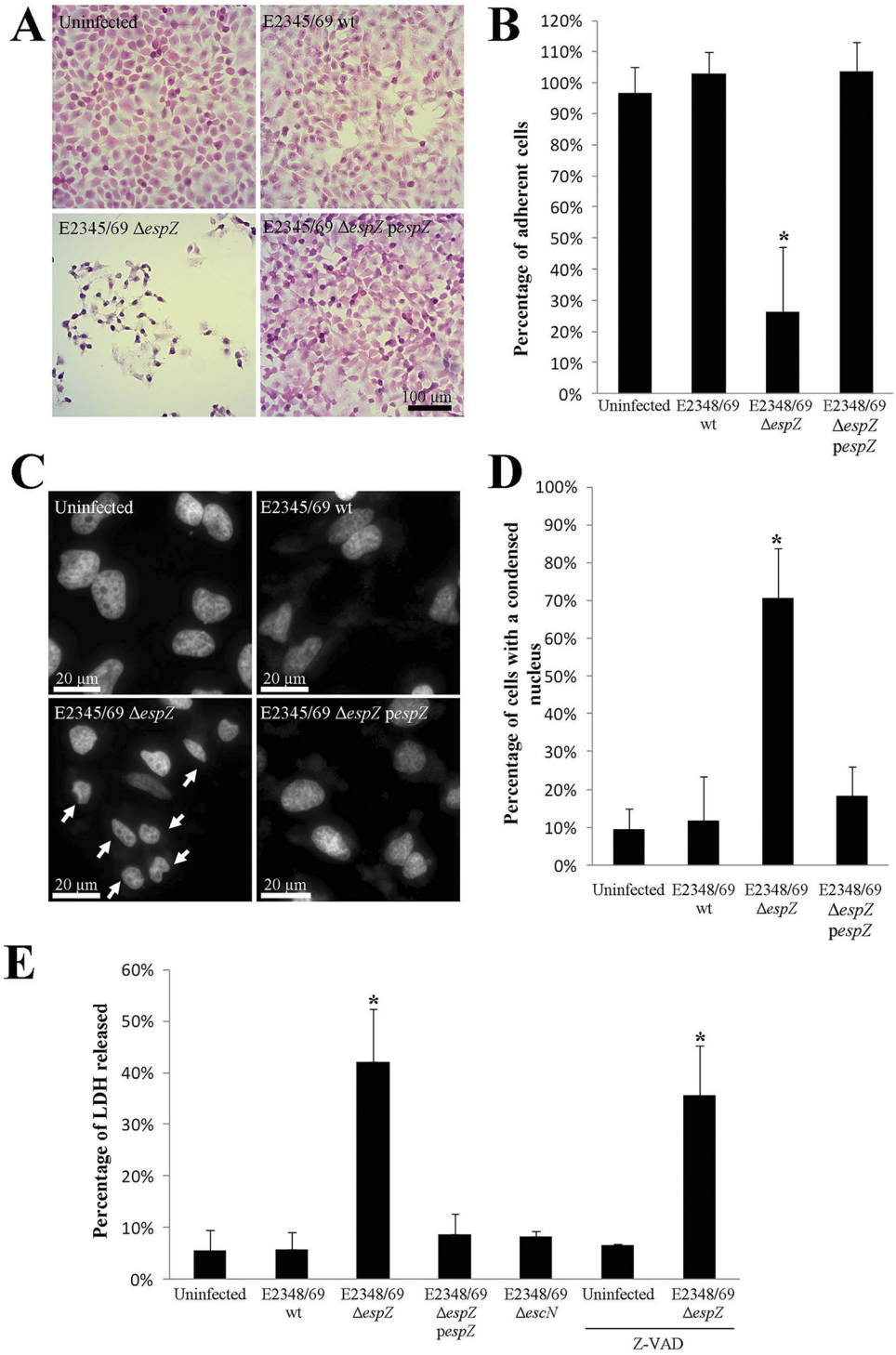

FIG 1 EPEC *espZ* mutant is cytotoxic. HeLa cells were infected with wild-type E2348/69, E2348/69 Δ*espZ*, and complemented E2348/69 Δ*espZ* p*espZ*. Uninfected cells were used as a control. Hematoxylin-and-eosin staining was used to visualize adherent cells 3 h postinfection (A), and Hoechst staining was used to visualize nuclei 1 h postinfection (C). Enumeration of the remaining cells 3 h postinfection revealed extensive cell detachment in monolayers infected with E2348/69 Δ*espZ* but not in the uninfected cells or cells infected with wild-type E2348/69 or E2348/69 Δ*espZ* complemented with *espZ*. Significant differences from uninfected cells are indicated by asterisks ($P < 0.01$) (B). While deletion of *espZ* induced nuclear condensation (white arrows), no difference was observed between cells infected with E2348/69 or E2348/69 Δ*espZ* complemented with *espZ* and uninfected cells (C). Using AxioVision software to enumerate cells with a condensed nucleus (<100 μm^2) (D) revealed a significant increase when cells were infected with E2348/69 Δ*espZ* compared to uninfected cells or cells infected with wild-type E2348/69 or E2348/69 Δ*espZ* complemented with *espZ*. Significant differences from uninfected cells are indicated by asterisks ($P < 0.01$). Cells were untreated or treated with 50 μM zVAD-FMK 30 min prior to infection with wild-type E2348/69, E2348/69 Δ*escN*, E2348/69 Δ*espZ*, and complemented E2348/69 Δ*espZ* (E). LDH release increased when cells were infected with E2348/69 Δ*espZ*. Significant differences from uninfected cells are indicated by asterisks ($P < 0.01$) (see also Fig. S1 and S2 in the supplemental material).

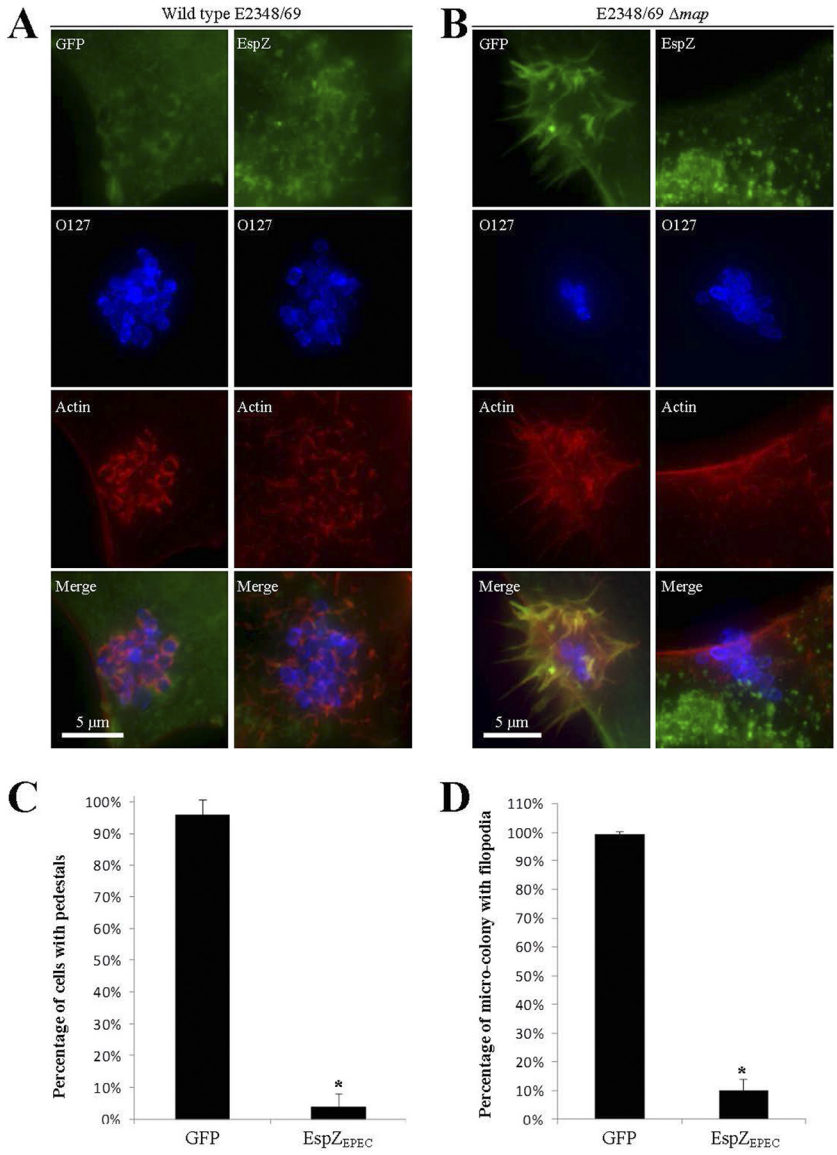

FIG 2 Cells ectopically expressing *espZ* are resistant to EPEC-induced pedestal and filopodium formation. HeLa-GFP and HeLa-EspZ cells were infected with wild-type E2348/69 (A) or E2348/69 Δ*map* overexpressing Map (B). Actin was stained with TRITC-phalloidin (red), the Myc-tagged EspZ with mouse anti-Myc (green), and EPEC with rabbit anti-O127 (blue). Transfected cells with pedestals (C) or with microcolony-associated filopodia (D) were quantified by immunofluorescence. One hundred cells were counted from three independent experiments. Results are means and SD. A large proportion of HeLa-GFP cells exhibited either pedestals or microcolony-associated filopodia, whereas neither pedestals nor filopodia were observed in HeLa-EspZ cells. Significant differences are indicated by asterisks ($P < 0.01$). Images are representative of three replicated experiments.

Ectopic expression of EspZ inhibits actin reorganization. To determine if ectopic expression of EspZ could protect cells from the cytotoxic effect induced by E2348/69 Δ*espZ*, we generated a eukaryotic expression vector (prK5-*myc-espZ*). As ectopically expressed EspZ was reported to be localized at the mitochondria (26), we first localized EspZ after ectopic expression of Myc-EspZ in HeLa cells (HeLa-EspZ). Immunofluorescence with anti-Myc antibodies revealed that EspZ was partially found at the plasma membrane (see Fig. S4A in the supplemental material). To confirm this result, plasma membranes of HeLa-EspZ cells were purified and analyzed by Western blotting (see Fig. S4B). This revealed that while the negative controls GADPH (cytoplasm marker) and cytochrome *c* (mitochondria) were undetectable, EspZ was partially present in the plasma membrane fraction.

HeLa-EspZ cells or HeLa cells expressing Myc-tagged green fluorescent protein (HeLa-GFP) were then infected for 1 h with wild-type E2348/69, E2348/69 Δ*espZ*, or the complemented mutant. DNA staining revealed that ectopic expression of EspZ blocked E2348/69 Δ*espZ* from inducing nuclear condensation (data not shown). This result suggests that ectopic expression of *espZ* inhibits cytotoxicity. Unexpectedly, although actin staining revealed the presence of microvillus-like processes (MLP) on HeLa-EspZ cells in the vicinity of adherent wild-type E2348/69 (Fig. 2A) and E2348/69 Δ*escN* (data not shown), confirming our previous observation of a T3SS-independent actin remodeling mechanism (27), formation of actin pedestals was evident in less than 5% of the HeLa-EspZ cells infected with wild-type E2348/69, compared with 80% of the infected HeLa-GFP cells (Fig. 2A and

C). In order to determine if this effect of EspZ was specific to Tir, HeLa-GFP and HeLa-EspZ cells were infected for 15 min with E2348/69 overexpressing Map, which induces extensive filopodium formation during the first 30 min of infection (28). Immunostaining and quantification revealed that less than 10% of microcolonies attached to the HeLa-EspZ cells were associated with filopodia. In contrast, filopodia were seen in almost 100% of the microcolonies attached to the HeLa-GFP cells (Fig. 2B and D). Importantly, we recently reported that ectopic expression of Map, EspM2, and EspT did not interfere with effector translocation (29), suggesting that the ability of EspZ to block translocation is specific.

EspZ inhibits effector translocation. To test the hypothesis that HeLa-EspZ cells are not permissive for translocation, we tracked effector translocation microscopically following infection with E2348/69 Δ*tir* expressing HA-tagged Tir, E2348/69 Δ*map* expressing HA-tagged Map, or E2348/69 Δ*espF* expressing FLAG-tagged EspF. Tir-HA staining outlined the attached bacteria in the control HeLa cells, but no HA staining was visible in HeLa-EspZ cells (Fig. 3A). Similarly, HA-tagged Map (see Fig. S5 in the supplemental material) and FLAG-tagged EspF (Fig. 3B) were found in the cytosol of HeLa but not HeLa-EspZ cells, suggesting that EspZ inhibits translocation of Tir, Map, and EspF. We further tested this hypothesis using the TEM1-β-lactamase translocation assay (30). HeLa and HeLa-EspZ cells were infected with E2348/69 expressing EspF or Tir fused to TEM1. E2348/69 Δ*escN* cells expressing EspF-TEM1 or Tir-TEM1 were used as negative controls. Translocation of Tir (Fig. 3C) and EspF (Fig. 3D) was significantly decreased in HeLa-EspZ cells compared to control HeLa cells. Neither effector was translocated from E2348/69 Δ*escN*. Notably, some translocation of Tir but not EspF could be detected in EspZ-transfected cells. This is likely due to the fact that not all the cells in the monolayers are transfected and to the greater Tir translocation efficiency. Taken together, these results suggest that EspZ inhibits translocation of T3SS effectors.

Shames et al. (4) reported that EspZ may influence the PI3K/Akt pathway. HeLa-GFP and HeLa-EspZ cells were treated for 30 min with the PI3K inhibitor LY-294002 and then infected with wild-type E2348/69; pedestal formation was used as a marker for protein translocation. No actin reorganization was seen in either untreated or LY-294002-treated HeLa-EspZ cells (see Fig. S6 in the supplemental material) compared to HeLa-GFP, suggesting that the PI3K/Akt pathway was not involved in EspZ-mediated inhibition of effector translocation.

EspZ blocks translocation from a second wave of EPEC infection. To determine if the cell toxicity observed with E2348/69 Δ*espZ* was due to constitutive effector translocation, we used the T3SS inhibitor protonophore CCCP (carbonyl cyanide *m*-chlorophenylhydrazone), which has been shown to hinder T3SS-mediated translocation from *Yersinia enterocolitica* (31) and *Shigella flexneri* (32). We first determined if CCCP blocks the T3SS of wild-type EPEC. Cells were infected with wild-type E2348/69 and treated either at the time of infection or 30 min later with CCCP. Untreated cells were used as a control. While pedestals were observed on untreated cells or cells treated with CCCP 30 min postinfection, MLPs in the absence of pedestals were observed on cells that were coinoculated with EPEC and CCCP (Fig. 4A). These results suggest that CCCP can block EPEC T3SS while not affecting cell signaling of already-translocated effectors. We next quantified the levels of LDH release in the absence or presence of CCCP. Infected cells were treated with CCCP 30 or 60 min following EPEC infection. Uninfected cells were used to control the level of LDH release induced by the CCCP itself. E2348/69 Δ*espZ* induced LDH release from the untreated cells or cells treated with CCCP 60 min after EPEC inoculation (Fig. 3B). In contrast, no LDH release was detected from cells treated with CCCP 30 min after E2348/69 Δ*espZ* inoculation. These results suggest that arresting protein translocation at 30 min postinfection protected cells from toxicity, while at 60 min the level went beyond the toxic threshold.

We recently showed that adherent EPEC bacteria block effector translocation from a second wave of EPEC infection in a T3SS-dependent manner (7). This result suggests that an effector injected by the first wave of EPEC infection is involved in arresting translocation of effectors expressed by the second EPEC wave (7). To determine if EspZ is involved in this phenotype, HeLa cells were either left uninfected or infected for 30 min with wild-type E2348/69, E2348/69 Δ*escV* (T3SS mutant), or E2348/69 Δ*espZ*. The cells were then superinfected with E2348/69 expressing Tir (Fig. 4C) or EspF (Fig. 4D) fused to TEM1, and the translocation dynamic was monitored. A decrease in Tir and EspF translocation was observed when the second wave of bacteria was used to infect cells preinfected with wild-type E2348/69. In contrast, no inhibition was seen when cells were preinfected with E2348/69 Δ*escV* or E2348/69 Δ*espZ* (Fig. 4C and D). These results further support the hypothesis that EspZ blocks effector protein translocation.

Inhibition of protein translocation is serotype specific. We next tested if EspZ from E2348/69 ($EspZ_{EPEC}$) can block effector translocation from other EPEC and EHEC strains. HeLa-GFP and HeLa-$EspZ_{EPEC}$ cells were infected with EPEC serotypes O103:H2, O111:H-, O55:H7, O55:H6, and EHEC O157:H7. Infection with E2348/69 (O127:H6) was used as a control, and pedestal formation was used as a marker for protein translocation. The number of infected cells with pedestals was quantified by epifluorescence (Fig. 5A). All the EPEC and EHEC strains formed typical pedestals upon infection of HeLa-GFP cells. In contrast, no pedestals were observed in HeLa-$EspZ_{EPEC}$ cells infected with E2348/69, EPEC O103:H2, O111:H− (Fig. 5B), or O55:H6. Importantly, EHEC O157:H7 and EPEC O55:H7, the progenitor of EHEC O157 (33), formed typical pedestals in the HeLa-$EspZ_{EPEC}$ cells (Fig. 5C). This result suggests that $EspZ_{EPEC}$ is unable to block effector translocation from these strains. A similar approach was applied to test the activity of EspZ from EHEC O157:H7 ($EspZ_{EHEC}$). Interestingly, we found that $EspZ_{EHEC}$ blocked the translocation from all the EPEC and EHEC strains tested and thus has a wider inhibitory range than $EspZ_{EPEC}$ (Fig. 5A to C).

The translocon plays no role in the strain-specific activity of EspZ. We previously reported that EspZ interacts with the pore-forming translocon component EspD (34). In order to determine if pore-forming proteins (EspD and EspB) or EspA (35) (which by forming EspA filaments links the translocation pore with the needle complex) plays a role in the observed strain specificity of EspZ, HeLa-GFP, HeLa-$EspZ_{EPEC}$, and HeLa-$EspZ_{EHEC}$ cells were infected with E2348/69 Δ*espB*, E2348/69 Δ*espD*, or E2348/69 Δ*espA* complemented with *espB*, *espD*, or *espA* from EPEC or from EHEC. All the strains formed actin pedestals in GFP-HeLa cells (data not shown), which confirmed that swapping the translocators between EPEC and EHEC did not interfere with the T3SS. Moreover, neither strain formed pedestals in HeLa-$EspZ_{EPEC}$ or

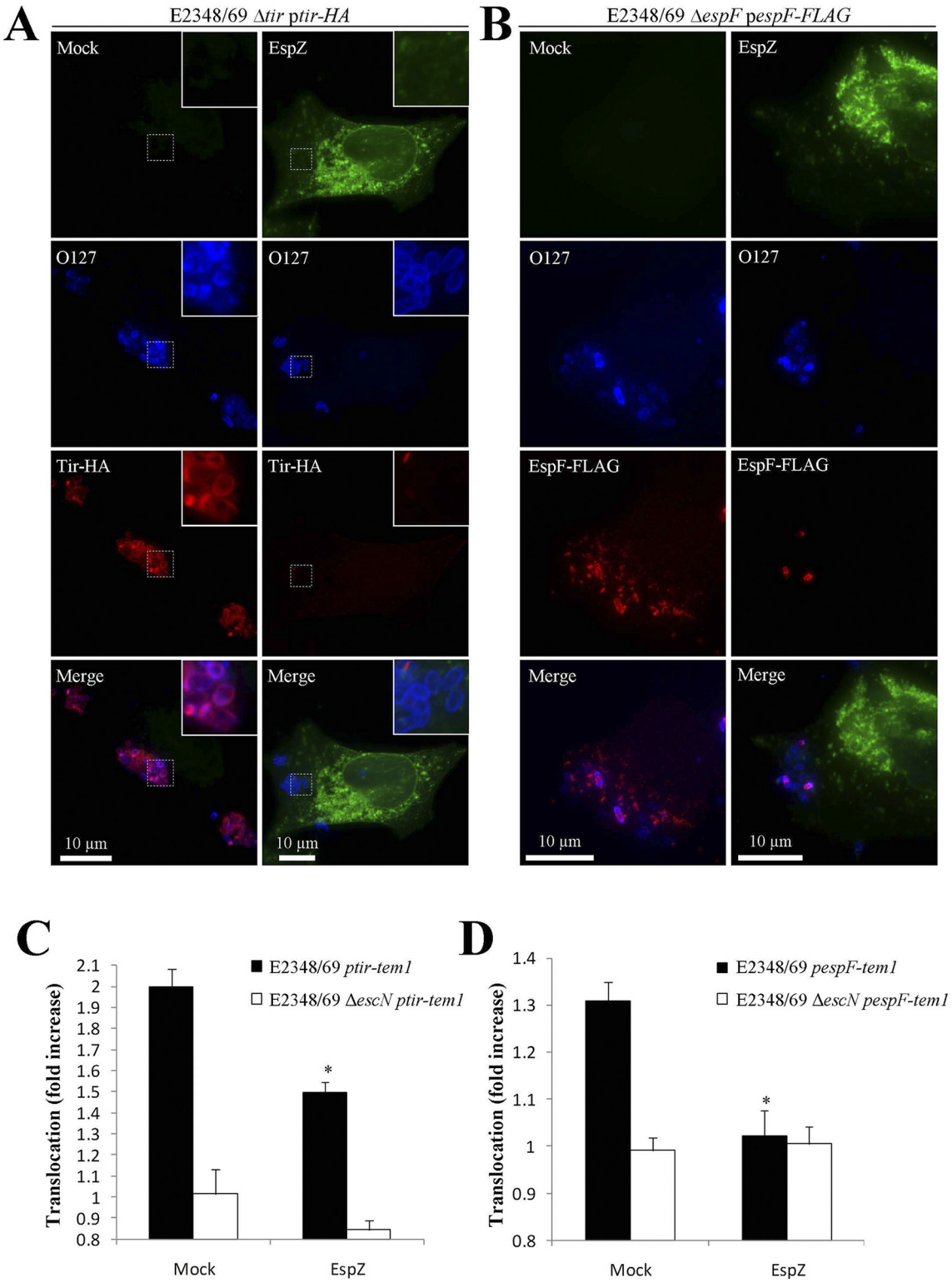

FIG 3 Ectopic expression of *espZ* blocks effector translocation. HeLa or HeLa-EspZ cells were infected with E2348/69 Δ*tir* expressing HA-tagged Tir (A), E2348/69 Δ*espF* expressing Flag-tagged EspF (B), E2348/69 expressing Tir-TEM (C), or E2348/69 expressing EspF-TEM (D). E2348/69 Δ*escN* bacteria expressing Tir-TEM or EspF-TEM fusions were used as negative controls. Myc-tagged EspZ was stained with mouse anti-Myc-FITC (green), HA-tagged and FLAG-tagged effectors with mouse anti-HA and mouse anti-Flag, respectively (red), and EPEC with rabbit anti-O127 (blue). Tir and EspF were detected in the pedestal and cytoplasm, respectively, in HeLa cells. In contrast, neither effector was detected in HeLa-EspZ cells. Images are representative of three replicated experiments. Translocation assays using TEM fusions showed that Tir and EspF were translocated into HeLa cells. Significantly reduced translocation was seen in HeLa-EspZ cells. No effector translocation was seen from the control strains. Results are the fold increase compared to uninfected cells from three independent experiments and are presented as means and SD (*, $P < 0.01$) (see also Fig. S5 in the supplemental material).

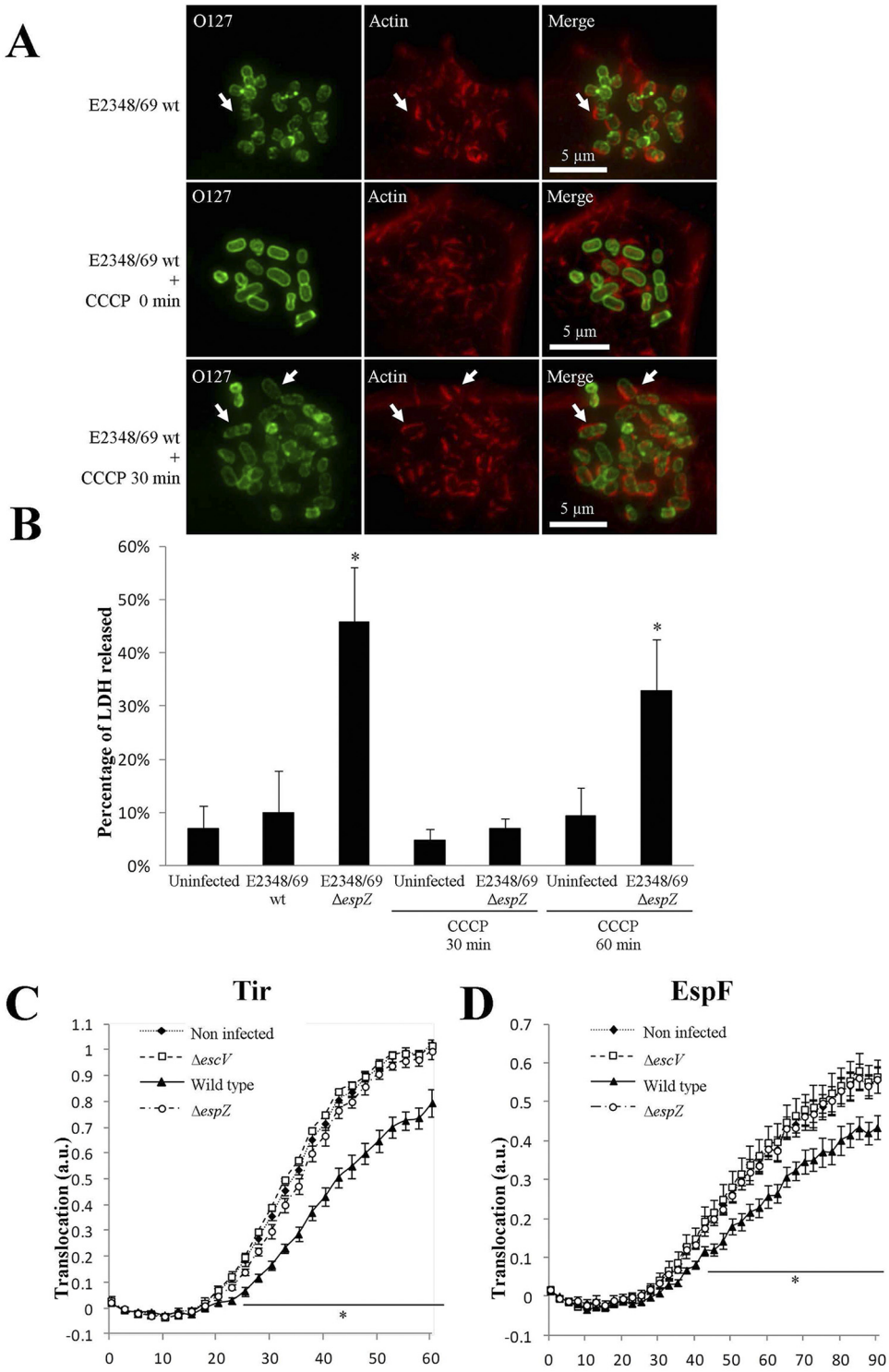

FIG 4 EspZ blocks effector translocation from a second EPEC infection wave. Cells were infected with wild-type E2348/69 or E2348/69 Δ*espZ* that was either untreated or treated with CCCP (carbonyl cyanide *m*-chlorophenylhydrazone) at the time of infection or 30 or 60 min postinfection. For immunofluorescence (A), actin was stained with TRITC-phalloidin (red) and EPEC with rabbit anti-O127 (green). LDH release (B) was measured after 2 h of infection. Treatment with CCCP, which inhibits the T3SS of EPEC, 30 min postinfection did not block pedestal formation (white arrows) but inhibited LDH release induced by E2348/69 Δ*espZ*. No inhibition of LDH release was observed in cells treated 60 min postinfection. Results are means and SD from three independent experiments (*, $P <$ 0.01). Cells were either left uninfected or infected with wild-type E2348/69, E2348/69 Δ*escV*, or E2348/69 Δ*espZ* and then superinfected with E2348/69 expressing Tir-TEM (C) or EspF-TEM fusions (D). Translocation of effectors by the second wave of bacteria was monitored using a real-time translocation assay on CCF2-preloaded cells. Translocation of Tir and EspF was reduced in cells preinfected with wild-type E2348/69. In contrast, similar translocation kinetics were recorded in uninfected control cells or cells infected with E2348/69 Δ*escV* or E2348/69 Δ*espZ*, suggesting that EspZ can block effector translocation of a second wave of infection. Results are means and SD from three independent experiments (*, $P < 0.01$).

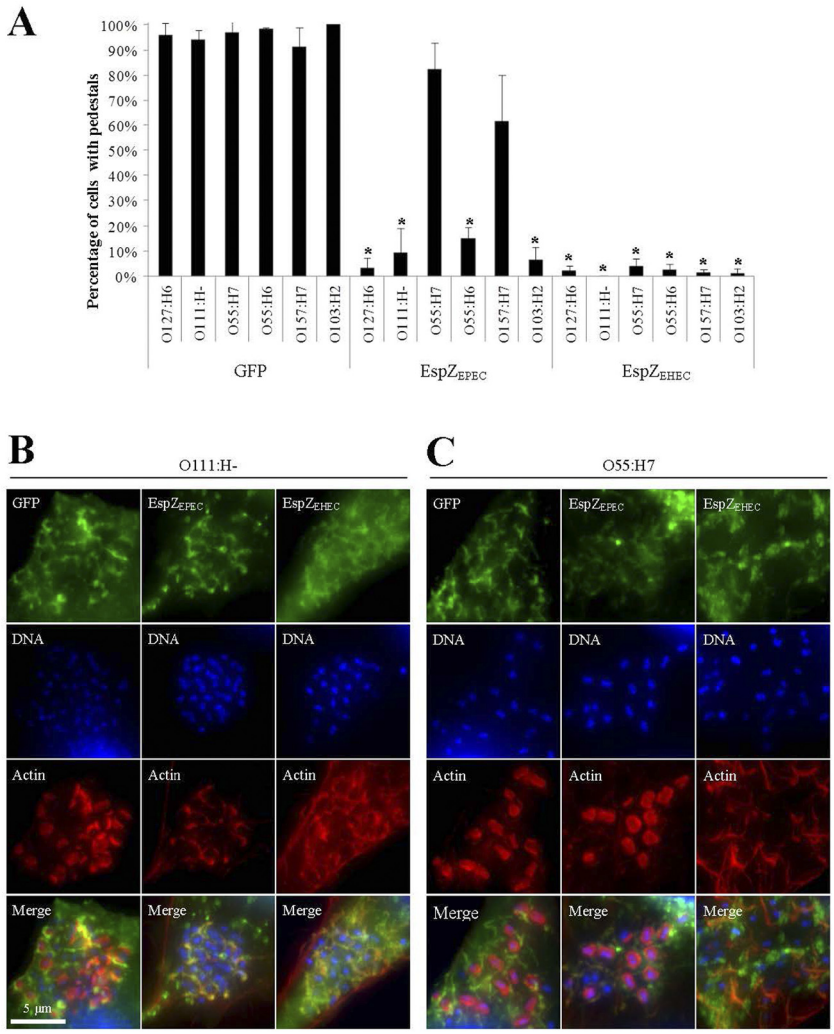

FIG 5 The activity of EspZ is serotype specific. HeLa-GFP, HeLa-EspZ$_{EPEC}$, or HeLa-EspZ$_{EHEC}$ cells were infected with EPEC strains E2348/69 (O127:H6) and B171 (O111:H−) (B), EPEC strains ICC219 (O57:H6), E22 (O103:H2), and ICC57 (O55:H7) (C), and EHEC 85-170 (O157:H7). Actin was stained with TRITC-phalloidin (red), Myc-tagged EspZ was detected with mouse anti-Myc (green), and DNA was detected with Hoechst (blue). Transfected cells with pedestals were quantified by immunofluorescence (A). One hundred cells were counted from five independent experiments. Results are means and SD. Pedestals were observed in HeLa-GFP and HeLa-EspZ$_{EPEC}$ cells infected with ICC57 or 85-170 (B). No pedestals were observed in HeLa-EspZ$_{EHEC}$ cells. Significant differences from HeLa-GFP cells are indicated by asterisks ($P < 0.01$).

HeLa-EspZ$_{EHEC}$ cells. These results suggest that EspB, EspD, and EspA are not involved in the strain-specific activity of EspZ.

In order to test if intimin, which is an outer membrane bacterial protein, cooperates with EspZ (which is exposed on the plasma membrane of infected cells) in determining host specificity, HeLa-GFP, HeLa-EspZ$_{EPEC}$, and HeLa-EspZ$_{EHEC}$ cells were infected with E2348/69 Δ*eae* complemented with *eae* (encoding intimin) from either EPEC or EHEC. All the strains formed actin pedestals in GFP-HeLa cells (data not shown), which confirmed that swapping the intimin between EPEC and EHEC did not interfere with the Tir signaling. Neither strain formed pedestals in HeLa-EspZ$_{EPEC}$ or HeLa-EspZ$_{EHEC}$ cells. These results suggest that intimin is not involved in the strain-specific activity of EspZ.

The extracellular loop of EspZ determines strain specificity. EspZ consists of 98 amino acids, comprising an N-terminal translocation signal, two TMDs and a 10-amino-acid extracellular loop (24). Alignment of EspZ orthologs showed that EspZ proteins from EHEC O157:H7 and EPEC O55:H7 are identical (see Fig. S7A in the supplemental material). However, little similarity was seen between the sequences of the extracellular loops (amino acids [aa] 65 to 74) of E2348/69 and EHEC O157:H7 (see Fig. S7A). In order to determine if the extracellular loop plays a role in EspZ specificity, we swapped the loops of EspZ$_{EPEC}$ and EspZ$_{EHEC}$ and tested the ability of the ectopically expressed recombinant EspZ variants to block translocation upon EPEC E2348/69 or EHEC O157:H7 infection. HeLa-GFP, HeLa-EspZ$_{EPEC}$, and HeLa-EspZ$_{EHEC}$ cells were used as controls and pedestal formation as a marker for protein translocation. The number of infected cells with pedestals was determined by epifluorescence. All the recombinant EspZ variants were able to inhibit pedestal formation by EPEC E2348/69 (see Fig. S7B). However, upon infection with EHEC O157:H7, normal pedestals and Tir staining were observed in cells expressing GFP, EspZ$_{EPEC}$, or EspZ$_{EHEC}$ with the EPEC loop (Fig. 6A). Importantly, inhibition of pedestal formation and

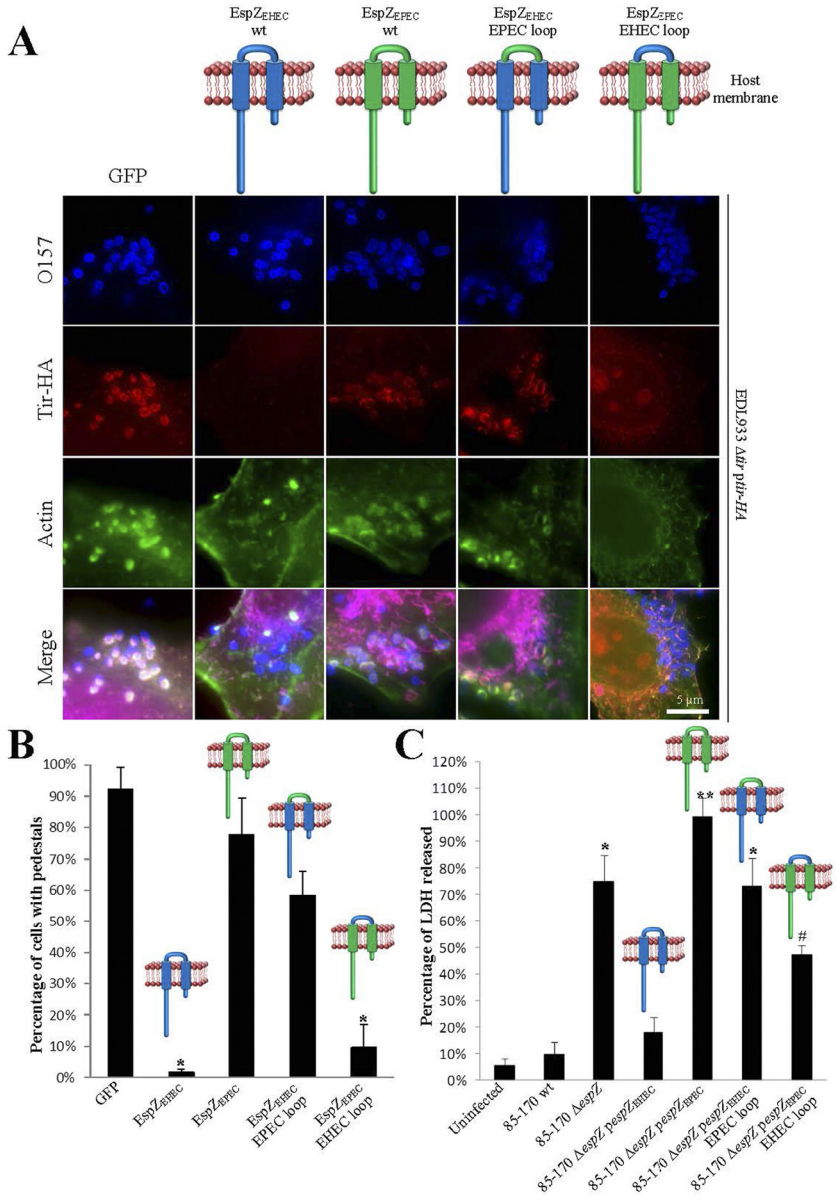

FIG 6 The extracellular loop of EspZ determines strain specificity. HeLa cells transfected with GFP, $EspZ_{EHEC}$, $EspZ_{EPEC}$, HeLa-$EspZ_{EHEC}$ with the EPEC loop, or $EspZ_{EPEC}$ with the EHEC loop were infected with EHEC EDL933 Δ*tir* expressing HA-tagged Tir (A). Actin was stained with RRX-phalloidin (red), HA-tagged Tir with mouse anti-Myc (green) and EPEC with rabbit anti-O157 (blue). Transfected cells with pedestals were quantified after immunofluorescence (B). One hundred cells were counted from five independent experiments. EHEC formed pedestals associated with Tir staining in HeLa-GFP, HeLa-$EspZ_{EPEC}$ or HeLa-$EspZ_{EHEC}$ with the loop of EPEC but not in HeLa-$EspZ_{EHEC}$ or HeLa-$EspZ_{EPEC}$ with the loop of EHEC. Results are presented as means ± SD. Significant differences from HeLa-GFP cells are indicated by asterisks ($P < 0.01$). (c) LDH release was measured from cells infected for 3 h with wild-type 85-170, 85-170 Δ*espZ*, or 85-170 Δ*espZ* expressing EHEC EspZ, EPEC EspZ, EHEC EspZ with the EPEC loop, or EPEC EspZ with the EHEC loop. LDH release increased when cells were infected with 85-170 Δ*espZ*, 85-170 Δ*espZ* expressing EPEC EspZ, or EHEC EspZ with the EPEC loop but not when cells were infected with 85-170 Δ*espZ* expressing EHEC EspZ. Partial complementation was observed with 85-170 Δ*espZ* expressing EHEC EspZ and EPEC EspZ with the EHEC loop. Significant differences from uninfected cells or from cells infected with 85-170 Δ*espZ* are indicated (* and #, respectively; $P < 0.01$) (see also Fig. S7 in the supplemental material).

no Tir staining was detected in cells expressing $EspZ_{EHEC}$ or $EspZ_{EPEC}$ with the EHEC loop (Fig. 6A and B). These results suggest that the extracellular loop of EspZ plays an important role in the strain-specific activity of EspZ.

In order to confirm that the loop swap does not alter the function of the proteins, HeLa cells were infected with wild-type E2348/69, E2348/69 Δ*espZ*, or E2348/69 Δ*espZ* expressing EPEC EspZ, EHEC EspZ, EPEC EspZ with the loop of EHEC, or EHEC EspZ with loop of EPEC. Cells infected with E2348/69 Δ*espZ* complemented with different mutants showed a level of LDH release similar to that of cells infected with wild-type E2348/69 (see Fig. S7C), confirming that the loop swap did not alter protein function in EPEC. HeLa cells were then infected with wild-type EHEC O157:H7 strain 85-170, 85-170 Δ*espZ*, and 85-170 Δ*espZ* express-

ing EPEC EspZ, EHEC EspZ, EPEC EspZ with the loop of EHEC, or EHEC EspZ with the loop of EPEC. As in EPEC, an EHEC Δ*espZ* mutant is highly toxic (exhibiting more than 70% of total LDH release) compare to wild-type EHEC (10% of total LDH release). Interestingly, whereas *espZ* from EHEC can complement 85-170 Δ*espZ*, no complementation was observed with 85-170 Δ*espZ* complemented with *espZ* from EPEC or with *espZ* from EHEC with the loop of EPEC. In contrast, 85-170 Δ*espZ* complemented with *espZ* from EPEC with the loop of EHEC showed partial complementation (Fig. 6C). Taken together, these results confirmed that the loop of EspZ play a major role in recognizing the infecting bacteria and inhibiting the T3SS.

DISCUSSION

T3SS effectors function in a coordinated manner. As effectors from a single pathogen can complement or antagonize each other, the timing and location of their activity, as well as their quantity, must be highly regulated. It is therefore not surprising that bacterial pathogens developed sophisticated mechanisms for spatial and temporal control of effector protein activity. Timing of effector gene expression provides a basic regulatory level, while T3SS chaperones assist in establishing an effector secretion hierarchy within the bacterial cell (7, 36). In EPEC, translocation efficiency is influenced by the effectors' steady-state levels in the bacteria and by two effector chaperones: CesF, which shows monospecificity for EspF (37), and CesT, which participates in the translocation of multiple effectors, including Tir, Map, EspH, and EspZ (38). The effectors' activity can also be regulated posttranslocation by mechanisms involving ubiquitination followed by proteasomal degradation (e.g., SopE [39]), protein phosphorylation (e.g., Tir [18]), or intracellular distribution via a specific hub (e.g., NleH, Map, and EspI, which all bind the membrane scaffold protein NHERF2 [40]).

Another level of regulation, involving a negative feedback loop on T3SS activity by an injected effector, was described for EPEC, *Yersinia*, and *Pseudomonas* (1, 7, 41). The identity of the involved EPEC effector remained elusive until now. In this study, we identified EspZ as the executor effector that mediates inhibition of effector translocation. Upon infection, we confirmed that an EPEC *espZ* mutant is highly toxic, probably due to a continuous translocation and effector overload. Cells ectopically expressing EspZ were refractory to effector protein translocation, as intracellular Map, Tir, and EspF were undetectable. Moreover, inhibition of T3SS by CCCP 30 min postinfection prevented cytotoxicity, while addition of the compound 60 min postinfection was not effective; suggesting that by 60 min the quantity of translocated effectors passed the cytotoxic threshold. This is consistent with the observation that the plasma membrane was permeabilized following infection with the *espZ* mutant between 30 and 60 min postinfection.

A *Citrobacter rodentium* (the mouse pathogen equivalent to EPEC [42]) *espZ* mutant is highly attenuated (6), suggesting that the control of effector translocation is key to successful colonization. Similarly, deletion of the *Yersinia* effector gene *yopK* (or *yopQ*) caused attenuation in a mouse model (43) and led to *in vitro* cytotoxicity (44). YopK/YopQ is a translocated cytosolic effector, which although contains no TMDs binds the pore-forming translocator YopB (45) and disrupts effector translocation (46). Interestingly, we previously reported that EspZ interacts with the EPEC pore-forming translocon component EspD (34). This interaction might play a role in the EspZ antitranslocation activity, although we have been unable thus far to coimmunoprecipitate EspZ and EspD (our unpublished results), possibly due to the small amount of EspD (as we were unable to detect EspD in cell lysates). Moreover, in *Yersinia* and *Pseudomonas*, the effectors YopE and ExoS have been implicated in translocation control via their Rho-GAP activity (1, 41). However, EspZ does not exhibit any similarity to ExoS or YopE and is unlikely to be a Rho-GAP, or a Rho-GAP-activation protein, since EspZ-expressing cells retain normal cytoskeletal organization. Based on the EspZ and YopK examples, it is likely that mechanisms controlling effector injection have been developed among bacteria employing T3SSs. However, in the absence of sequence or structural similarities between YopK and EspZ, the identity of the functionally conserved effectors in other bacteria is not easy to discover.

Recently, Shames et al. showed that EspZ interacts with the membrane host cell protein CD98 (4). However, as the knockdown of this protein did not alter the function of EspZ during infection (4), CD98 does not appear to play a role in the modulation of effector protein translocation. Uniquely, we found that the extracellular loop of EspZ has a sensor-like activity, which mediates strain specificity. While recombinant EspZ displaying the loop of EPEC does not inhibit effector translocation from EHEC O157:H7 and EPEC O55:H7, the loop of EHEC has a global activity, as it can inhibit protein translocation from all EPEC and EHEC strains. How EspZ mediates its negative effect on the T3SS activity is not clear yet, although a mechanism involving a specific timing might be involved. Nevertheless, by analogy with the loop of Tir that binds intimin on the bacterial outer membrane (26), our results indicate that the exposed loop of EspZ might interact with a secreted protein and/or with a bacterial outer membrane protein.

Based on our data, we can now suggest a model (see Fig. S8 in the supplemental material) in which, following infection, EspZ is translocated and integrated in a hairpin loop topology into the host cell plasma membrane. Then, by interacting with a strain-specific, presumably exposed, protein, the extracellular loop of EspZ transduces a signal (e.g., conformation change) to its N terminus, which by interacting with EspD (a component of the translocation pore) arrests further effector translocation.

In summary, in this study we identified a novel T3SS EPEC/EHEC effector that maintains the viability of infected cells by gauging the duration of effector protein translocation via caspase- and PI3K/Akt-independent mechanisms. This regulation is essential for successful colonization and infection. Understanding how EspZ inhibits T3SS might lead to the development of new strategies to control human and animal EPEC and EHEC infection and carriage.

MATERIALS AND METHODS

Bacterial strains. The *E. coli* strains used in this study are listed in Table S1 in the supplemental material. EPEC was cultured in LB broth at 37°C for 18 h with the appropriate antibiotics. Overnight cultures were diluted 1:100 in DMEM with low glucose (1,000 mg/liter) and grown for 3 h at 37°C without agitation. EHEC was directly cultured in DMEM with low glucose and grown overnight at 37°C without agitation. Cells in 24-well plates were infected with 25 μl of overnight cultures. Isopropyl-β-d-thiogalactopyranoside (1 mM) was added for 30 min when needed.

Molecular biology techniques. The plasmids and primers used in this study are listed in Table S1 in the supplemental material. *espZ* was deleted from EPEC strain E2348/69 and EHEC strain 85-170 using the lambda red

system (47), generating strains ICC829 and ICC831, respectively. Primer pairs F11/R11 (deletion for EPEC) and F11/R17 (deletion for EHEC) were used to amplify the kanamycin cassette in pKD4. Primers F12/R12 and F13/R13 were used to confirm the deletion in EPEC and F18/R18 was used to confirm the deletion in EHEC. *espZ* was cloned into the bacterial expression vector pSA10 (48) following amplification from E2348/69 and EDL933 genomic DNA using primer pair F1/R1 and primer pair F20/R20, respectively. The PCR products were cloned into the EcoRI/SmaI sites of pSA10, generating plasmids pICC1101 and pICC1111, respectively. The *espZ* 4-HA tag was generated by inverse PCR using sequential PCRs from pICC1101 with primers F2/R2, F3/R3, and F4/R4, generating plasmid pICC1100. *myc*-tagged *espZ* was generated by inverse PCR from pICC1101 with primer pair F19/R19, generating plasmid pICC1108. Mutation of the loop with an HA tag was generated by inverse PCR from pICC1101 with primer pair F20/R20, generating plasmid pICC1109. A Tir-HA tag-expressing vector was obtained by amplification of *tir* from EHEC TUV 93-0 genomic DNA as the template using primer pair F6/R6 and cloning into the SmaI/PstI sites of pSA10, generating plasmid pICC1102. HA-tagged *map* was generated by inverse PCR using pSA10-map (49) with primers F5 and R5, generating plasmid pICC1103. Pore protein EspD was cloned into the bacterial expression vector pBAD/Myc-His-C (Invitrogen) following amplification from E2348/69 and EDL933 genomic DNA using primer pairs F14/R14 and F15/R15. The PCR product was cloned into the NcoI/EcoRI and NcoI/BglII sites of pBAD, generating plasmids pICC882 and pICC867. *espB* was cloned into the NcoI/BglII sites of the bacterial expression vector pBAD following amplification using primer pair F16/R16 and E2348/69 genomic DNA as the template, generating plasmid pICC881. For cloning into a eukaryotic expression vector, the *espZ* genes from EPEC and EHEC were amplified from E2348/69 and EDL933 genomic DNA using primers F7/R7 and F8/R8, respectively. The PCR products were cloned into the BamHI/EcoRI sites of pRK5-*myc*, generating plasmids pICC1104 and pICC1105. The extracellular *espZ* loops were exchanged by inverse PCR using primer pairs F9/R9 and F10/R10 with pICC1101, pICC1104, pICC1105, and pICC1111 as the templates, generating plasmids pICC1112, pICC1106, pICC07, and pICC1113.

Tissue culture and transfection. HeLa cells were grown at 37°C in a 5% CO_2 atmosphere in DMEM supplemented with 10% (vol/vol) heat-inactivated fetal calf serum (Invitrogen), nonessential amino acids (Sigma), and 2 mM Glutamax (Invitrogen). Cells were transfected with Fugene-6 (Roche) or GeneJuice (Merck) according to the manufacturer's recommendations. The global caspase inhibitor zVAD-FMK (Promega) was used at a final concentration of 50 μM. The protonophore carbonyl cyanide *m*-chlorophenylhydrazone (CCCP; Sigma) was used at a final concentration of 25 μM.

Cell detachment assay. HeLa cells were seeded in 24-well plates. After 48 h, confluent cells were infected with primed bacteria for 1 h. Cells were then washed five times with PBS every hour. After 3 h of infection, cells were trypsinized and counted using a Malassez counting chamber. To visualize cells after the infection, monolayers on coverslips were fixed with paraformaldehyde (PFA) for 15 min, immersed in Harris hematoxylin solution for 15 s, and subsequently washed with water until they appeared blue. They were next treated with a 1% eosin solution for 5 s and briefly rinsed with water. Coverslips were then mounted and observed with a light microscope (Zeiss).

LDH release assay. HeLa cells were seeded in 24-well plates. After 48 h, confluent cells were infected with primed bacteria for 1 h. Cells were then washed five times with PBS and incubated with DMEM without dye for one additional hour. Cell supernatants were then harvested, and the LDH released was measured using a CytoTox 96 nonradioactive cytotoxicity assay (Promega). The percentage of LDH released is calculated as the amount of LDH measured in the supernatant divided by the total amount of LDH.

***β*-Lactamase (TEM-1) translocation assay.** HeLa cells were seeded in 96-well plates and transfected the following day. After 24 h, confluent cells were infected with primed wild-type E2348/69 or E2348/69 Δ*escN* bacteria expressing either the Tir- or EspF-TEM1-fusion. The translocation assay was performed as described previously (50).

Two-wave infection. The two-wave infection was conducted as described by Mills et al. (7). Briefly, HeLa cells were seeded in 96-well plates at a density of 3×10^4 cells/well. The following day, cells were incubated with 1 μM CCF2/AM (Invitrogen) and 2.5 mM probenecid for 1 h in the dark at room temperature and then for 15 min at 37°C before being infected for 30 min with the first wave of primed bacteria (Casamino Acids-DMEM [CDMEM] supplemented with 2.5 mM probenecid). Following the first wave of infection, cells were washed gently with CDMEM supplemented with probenecid and reinfected with the second wave of bacterial cultures. Immediately upon infection, the plates were placed in a plate reader (Spectrafluor Plus; Tecan) set at 37°C, and thus the infection process took place in the plate reader. Cells were excited at 405 nm, and emission at 465 nm and 535 nm was recorded at 150-s intervals.

Immunofluorescence microscopy. Cells were grown in 24-well cell culture plates to 60 to 70% confluence. Monolayers were treated, infected, and stained as described before (28). The coverslips were mounted in ProLong Gold antifading agent (Invitrogen) and examined by conventional epifluorescence microscopy using a Zeiss Axioimager microscope. Deconvolution of the images was done with AxioVision LE re software (Zeiss); the slice of interest was projected to form the new image.

Actin was detected with Oregon green phalloidin (Invitrogen) or TRITC (tetramethyl rhodamine isocyanate) phalloidin (Sigma). Bacteria were labeled with polyclonal anti-O127 and anti-O157 antibody (kindly provided by Roberto La Ragione, Veterinary Laboratory Agency, United Kingdom). Myc-tagged, HA-tagged, and FLAG-tagged proteins were labeled with monoclonal anti-Myc (Millipore), monoclonal anti-HA (Cambridge Bioscience), or TRITC–conjugated monoclonal anti-HA (Sigma) or monoclonal anti-FLAG (Sigma). AMCA-, Cy2-, RRX-, or Cy5-conjugated donkey anti-mouse and anti-rabbit antibodies (Jackson ImmunoResearch) were used as secondary antibodies. DNA was stained using Hoechst (Sigma).

Statistical analysis. All experiments were conducted in triplicate and repeated at least three times. Results were expressed as means ± standard deviations (SD). The statistical significance was determined by two-way analysis of variance (ANOVA) (GraphPad PRISM software), and a *P* value of <0.01 was considered significant.

SUPPLEMENTAL MATERIAL

Supplemental material for this article may be found at http://mbio.asm.org/lookup/suppl/doi:10.1128/mBio.00317-12/-/DCSupplemental.

Text S1, DOCX file, 0.1 MB.
Figure S1, DOCX file, 5 MB.
Figure S2, DOCX file, 0.7 MB.
Figure S3, DOCX file, 3.1 MB.
Figure S4, DOCX file, 1.7 MB.
Figure S5, DOCX file, 1.8 MB.
Figure S6, DOCX file, 0.8 MB.
Figure S7, DOCX file, 4 MB.
Figure S8, DOCX file, 1.5 MB.
Table S1, DOCX file, 0.1 MB.

ACKNOWLEDGMENTS

This work was supported by grants from the Israel Science Foundation (I. R.) and the Wellcome Trust (G.F.)

REFERENCES

1. **Aili M, et al.** 2008. Regulation of *Yersinia* Yop-effector delivery by translocated YopE. Int. J. Med. Microbiol. **298**:183–192.
2. **Erhardt M, Namba K, Hughes KT.** 2010. Bacterial nanomachines: the flagellum and type III injectisome. Cold Spring Harb. Perspect. Biol. **2**:a000299.
3. **Cornelis GR.** 2010. The type III secretion injectisome, a complex nanomachine for intracellular "toxin" delivery. Biol. Chem. **391**:745–751.
4. **Shames SR, et al.** 2010. The pathogenic *E. coli* type III effector EspZ

interacts with host CD98 and facilitates host cell prosurvival signalling. Cell. Microbiol. **12**:1322–1339.
5. **Laaberki MH, Janabi N, Oswald E, Repoila F.** 2006. Concert of regulators to switch on LEE expression in enterohemorrhagic *Escherichia coli* O157:H7: interplay between Ler, GrlA, HNS and RpoS. Int. J. Med. Microbiol. **296**:197–210.
6. **Deng W, et al.** 2004. Dissecting virulence: systematic and functional analyses of a pathogenicity island. Proc. Natl. Acad. Sci. U. S. A. **101**: 3597–3602.
7. **Mills E, Baruch K, Charpentier X, Kobi S, Rosenshine I.** 2008. Real-time analysis of effector translocation by the type III secretion system of enteropathogenic *Escherichia coli*. Cell Host Microbe **3**:104–113.
8. **Chen HD, Frankel G.** 2005. Enteropathogenic *Escherichia coli*: unravelling pathogenesis. FEMS Microbiol. Rev. **29**:83–98.
9. **Pennington H.** 2010. *Escherichia coli* O157. Lancet **376**:1428–1435.
10. **Frankel G, Phillips AD.** 2008. Attaching effacing *Escherichia coli* and paradigms of tir-triggered actin polymerization: getting off the pedestal. Cell. Microbiol. **10**:549–556.
11. **Frankel G, et al.** 1998. Enteropathogenic and enterohaemorrhagic *Escherichia coli*: more subversive elements. Mol. Microbiol. **30**:911–921.
12. **McDaniel TK, Jarvis KG, Donnenberg MS, Kaper JB.** 1995. A genetic locus of enterocyte effacement conserved among diverse enterobacterial pathogens. Proc. Natl. Acad. Sci. U. S. A. **92**:1664–1668.
13. **Jerse AE, Yu J, Tall BD, Kaper JB.** 1990. A genetic locus of enteropathogenic *Escherichia coli* necessary for the production of attaching and effacing lesions on tissue culture cells. Proc. Natl. Acad. Sci. U. S. A. **87**:7839–7843.
14. **Jarvis KG, et al.** 1995. Enteropathogenic *Escherichia coli* contains a putative type-III secretion system necessary for the export of proteins involved in attaching and effacing lesion formation. Proc. Natl. Acad. Sci. U. S. A. **92**:7996–8000.
15. **Jarvis KG, Kaper JB.** 1996. Secretion of extracellular proteins by enterohemorrhagic *Escherichia coli* via a putative type III secretion system. Infect. Immun. **64**:4826–4829.
16. **Kenny B, Finlay BB.** 1995. Protein secretion by enteropathogenic *Escherichia coli* is essential for transducing signals to epithelial-cells. Proc. Natl. Acad. Sci. U. S. A. **92**:7991–7995.
17. **Wong AR, et al.** 2011. Enteropathogenic and enterohaemorrhagic *Escherichia coli*: even more subversive elements. Mol. Microbiol. **80**: 1420–1438.
18. **Kenny B, et al.** 1997. Enteropathogenic *E. coli* (EPEC) transfers its receptor for intimate adherence into mammalian cells. Cell **91**:511–520.
19. **Liu H, Magoun L, Luperchio S, Schauer DB, Leong JM.** 1999. The tir-binding region of enterohaemorrhagic *Escherichia coli* intimin is sufficient to trigger actin condensation after bacterial-induced host cell signalling. Mol. Microbiol. **34**:67–81.
20. **Kenny B, et al.** 2002. Co-ordinate regulation of distinct host cell signalling pathways by multifunctional enteropathogenic *Escherichia coli* effector molecules. Mol. Microbiol. **44**:1095–1107.
21. **Tu X, Nisan I, Yona C, Hanski E, Rosenshine I.** 2003. EspH, a new cytoskeleton-modulating effector of enterohaemorrhagic and enteropathogenic *Escherichia coli*. Mol. Microbiol. **47**:595–606.
22. **Papatheodorou P, et al.** 2006. The enteropathogenic *Escherichia coli* (EPEC) map effector is imported into the mitochondrial matrix by the TOM/Hsp70 system and alters organelle morphology. Cell. Microbiol. **8**:677–689.
23. **Tobe T, et al.** 2006. An extensive repertoire of type III secretion effectors in *Escherichia coli* O157 and the role of lambdoid phages in their dissemination. Proc. Natl. Acad. Sci. U. S. A. **103**:14941–14946.
24. **Kanack KJ, Crawford JA, Tatsuno I, Karmali MA, Kaper JB.** 2005. SepZ/EspZ is secreted and translocated into HeLa cells by the enteropathogenic *Escherichia coli* type III secretion system. Infect. Immun. **73**: 4327–4337.
25. **Crawford JA, Kaper JB.** 2002. The N-terminus of enteropathogenic *Escherichia coli* (EPEC) tir mediates transport across bacterial and eukaryotic cell membranes. Mol. Microbiol. **46**:855–868.
26. **Shames SR, Croxen MA, Deng W, Finlay BB.** 2011. The type III system-secreted effector EspZ localizes to host mitochondria and interacts with the translocase of inner mitochondrial membrane 17b. Infect. Immun. **79**:4784–4790.
27. **Phillips AD, Giròn J, Hicks S, Dougan G, Frankel G.** 2000. Intimin from enteropathogenic *Escherichia coli* mediates remodelling of the eukaryotic cell surface. Microbiology **146**:1333–1344.
28. **Berger CN, Crepin VF, Jepson MA, Arbeloa A, Frankel G.** 2009. The mechanisms used by enteropathogenic *Escherichia coli* to control filopodia dynamics. Cell. Microbiol. **11**:309–322.
29. **Wong AR, Clements A, Raymond B, Crepin VF, Frankel G.** 2012. The interplay between the *Escherichia coli* Rho guanine nucleotide exchange factor effectors and the mammalian RhoGEF inhibitor EspH. mBio **3**:e00250-11.
30. **Charpentier X, Oswald E.** 2004. Identification of the secretion and translocation domain of the enteropathogenic and enterohemorrhagic *Escherichia coli* effector Cif, using TEM-1 beta-lactamase as a new fluorescence-based reporter. J. Bacteriol. **186**:5486–5495.
31. **Wilharm G, et al.** 2004. *Yersinia enterocolitica* type III secretion depends on the proton motive force but not on the flagellar motor components MotA and MotB. Infect. Immun. **72**:4004–4009.
32. **Schroeder GN, Jann NJ, Hilbi H.** 2007. Intracellular type III secretion by cytoplasmic *Shigella flexneri* promotes caspase-1-dependent macrophage cell death. Microbiology **153**:2862–2876.
33. **Leopold SR, Shaikh N, Tarr PI.** 2010. Further evidence of constrained radiation in the evolution of pathogenic *Escherichia coli* O157:H7. Infect. Genet. Evol. **10**:1282–1285.
34. **Creasey EA, Delahay RM, Daniell SJ, Frankel G.** 2003. Yeast two-hybrid system survey of interactions between LEE-encoded proteins of enteropathogenic *Escherichia coli*. Microbiology **149**:2093–2106.
35. **Knutton S, et al.** 1998. A novel EspA-associated surface organelle of enteropathogenic *Escherichia coli* involved in protein translocation into epithelial cells. EMBO J. **17**:2166–2176.
36. **Wang D, Roe AJ, McAteer S, Shipston MJ, Gally DL.** 2008. Hierarchal type III secretion of translocators and effectors from *Escherichia coli* O157:H7 requires the carboxy terminus of SepL that binds to tir. Mol. Microbiol. **69**:1499–1512.
37. **Elliott SJ, et al.** 2002. A gene from the locus of enterocyte effacement that is required for enteropathogenic *Escherichia coli* to increase tight-junction permeability encodes a chaperone for EspF. Infect. Immun. **70**: 2271–2277.
38. **Thomas NA, et al.** 2005. CesT is a multi-effector chaperone and recruitment factor required for the efficient type III secretion of both LEE- and non-LEE-encoded effectors of enteropathogenic *Escherichia coli*. Mol. Microbiol. **57**:1762–1779.
39. **Kubori T, Galán JE.** 2003. Temporal regulation of *salmonella* virulence effector function by proteasome-dependent protein degradation. Cell **115**:333–342.
40. **Martinez E, et al.** 2010. Binding to Na(+) /H(+) exchanger regulatory factor 2 (NHERF2) affects trafficking and function of the enteropathogenic *Escherichia coli* type III secretion system effectors map, EspI and NleH. Cell. Microbiol. **12**:1718–1731.
41. **Cisz M, Lee PC, Rietsch A.** 2008. ExoS controls the cell contact-mediated switch to effector secretion in *Pseudomonas aeruginosa*. J. Bacteriol. **190**: 2726–2738.
42. **Mundy R, MacDonald TT, Dougan G, Frankel G, Wiles S.** 2005. *Citrobacter rodentium* of mice and man. Cell. Microbiol. **7**:1697–1706.
43. **Holmström A, Rosqvist R, Wolf-Watz H, Forsberg A.** 1995. Virulence plasmid-encoded YopK is essential for *Yersinia pseudotuberculosis* to cause systemic infection in mice. Infect. Immun. **63**:2269–2276.
44. **Holmström A, et al.** 1997. YopK of *Yersinia pseudotuberculosis* controls translocation of Yop effectors across the eukaryotic cell membrane. Mol. Microbiol. **24**:73–91.
45. **Brodsky IE, et al.** 2010. A *Yersinia* effector protein promotes virulence by preventing inflammasome recognition of the type III secretion system. Cell Host Microbe **7**:376–387.
46. **Dewoody R, Merritt PM, Houppert AS, Marketon MM.** 2011. YopK regulates the *Yersinia pestis* type III secretion system from within host cells. Mol. Microbiol. **79**:1445–1461.
47. **Datsenko KA, Wanner BL.** 2000. One-step inactivation of chromosomal genes in *Escherichia coli* K-12 using PCR products. Proc. Natl. Acad. Sci. U. S. A. **97**:6640–6645.
48. **Schlosser-Silverman E, Elgrably-Weiss M, Rosenshine I, Kohen R, Altuvia S.** 2000. Characterization of *Escherichia coli* DNA lesions generated within J774 macrophages. J. Bacteriol. **182**:5225–5230.
49. **Simpson N, et al.** 2006. The enteropathogenic *Escherichia coli* type III secretion system effector map binds EBP50/NHERF1: implication for cell signalling and diarrhoea. Mol. Microbiol. **60**:349–363.
50. **Munera D, Crepin VF, Marches O, Frankel G.** 2010. N-terminal type III secretion signal of enteropathogenic *Escherichia coli* translocator proteins. J. Bacteriol. **192**:3534–3539.